

Showcasing research from Professor Huanwen Chen's laboratory, Jiangxi Key Laboratory for Mass Spectrometry and Instrumentation, East China University of Technology, Nanchang, China.

Rapid detection of metal impurities on the surfaces of intact objects with irregular shapes using electrochemical mass spectrometry

An electrochemical mass spectrometry method has been developed for inspection of metal impurities on the surfaces of intact objects with irregular shapes. An intact object was immersed in a flow cell at appropriate potentials to form metal ions, followed by detection with online ESI-MS. This method has the advantages of high speed, high sensitivity and minimal invasiveness, and can be used for analysis of samples where physical methods are difficult or lead to destruction of the sample

As featured in:





See Huanwen Chen et al., *Analyst*, 2019, 144, 3505.



Cite this: *Analyst*, 2019, **144**, 3505

## Rapid detection of metal impurities on the surfaces of intact objects with irregular shapes using electrochemical mass spectrometry†

Lili Song, Jiaquan Xu,  Dacai Zhong, Konstantin Chingin,  Ying Qu and Huanwen Chen\*

New approaches are demanded in daily life and industry for the rapid inspection of chemical impurities on various objects, particularly those with irregular shapes. Herein, an analytical strategy combining electrochemistry (EC) and mass spectrometry (MS) has been developed for the direct inspection of metal impurities on various objects which are commonly used in daily life and industry. An intact object (e.g., necklace, bearing, ring) was immersed in an electrolytic cell containing EDTA/acetonitrile/water solution at appropriate potentials to form metal ions. The formed metal ions were instantly chelated with specific ligands (e.g. ethylenediaminetetraacetic acid) and sampled for online electrospray ionization (ESI) with high-resolution MS detection. The unique feature of the method is that metal speciation information can be obtained even when just a metal impurity (e.g., Pb, Ni) is localized on a hard-to-reach tiny spot on the inner surface of objects with extremely irregular shapes. A single sample analysis requires less than 10 minutes, regardless of the object shape. The limit of detection is 0.05 ppb with sample consumption on the nanogram level. The experimental results demonstrate that the method is promising for the non-destructive quality and safety inspection of metal impurities on virtually any kinds of objects with high chemical sensitivity.

Received 21st December 2018,  
Accepted 26th March 2019

DOI: 10.1039/c8an02472c

rsc.li/analyst

## 1 Introduction

Metals (e.g., Au, Ag, Pt) are ubiquitous in daily life objects (e.g., in precious jewelry, pans, pots), industry (e.g., in bearings, spark plugs, fuel nozzles) and research activities (e.g., in catalysts, biomaterials or nanomaterials).<sup>1–4</sup> Some metal impurities on surfaces of objects are harmful to health and can easily leak out into the environment.<sup>5,6</sup> For example, Cu and Ni are normally doped into pure gold to fabricate K-gold, and the doping of Pb in Au jewelry can cause health problems.<sup>7–9</sup> Thus, the versatile and rapid detection of the metal components on objects with various shapes is of great significance for quality and safety inspection.

At present, metal or metal ions are normally sampled from the objects and then digested using various chemical reagents to form analyte solutions. The solutions are analyzed offline by atomic absorption spectrometry (AAS),<sup>10,11</sup> atomic emission spectrometry (OES)<sup>12,13</sup> or inductively coupled plasma mass

spectrometry (ICP-MS).<sup>14</sup> These methods are mature and stable but require a significantly long time for sample manipulation and pretreatment, resulting in a low analytical throughput.<sup>15</sup> Laser ablation inductively coupled plasma mass spectrometry (LA-ICP-MS)<sup>16–18</sup> and electrospray laser desorption ionization mass spectrometry<sup>19</sup> have been attempted for online metal analysis, but the substantial complication associated with these methods is the requirement of solid standards with similar composition to sample for quantitative analysis. X-ray fluorescence is an *in situ* and non-destructive method for metal analysis,<sup>20–22</sup> but is not very accurate for trace analysis. Besides this, LA-ICP-MS, LA-ESI-MS and X-ray fluorescence are only suitable as micro-area analysis methods and are unsuitable for the rapid analysis of total metal impurities on macro-sized intact objects, particularly on those with irregular shapes due to the directivity of the rays.

Electrochemistry coupled with mass spectrometry (EC/MS) is a powerful method for the elucidation of redox reaction mechanisms and many valuable bioanalytical applications.<sup>23</sup> In EC/MS, MS can serve as a detector for electrochemical cells, providing information about electrochemical reactions.<sup>24,25</sup> On the other hand, electrochemical conversion can be used to improve analyte ionization or provide modification to the analyte prior to MS analysis,<sup>26</sup> such as online chemical

Jiangxi Key Laboratory for Mass Spectrometry and Instrumentation,  
East China University of Technology, Nanchang 330013, P. R. China.

E-mail: chw8868@gmail.com

†Electronic supplementary information (ESI) available. See DOI: 10.1039/c8an02472c

tagging<sup>27</sup> and protein oxidative cleavage.<sup>28</sup> Herein, a method was developed for the rapid quality and safety inspection of metal impurities on the whole surfaces of intact objects with irregular shapes using electrochemical mass spectrometry. Metal on the sample surface is transformed into metal ions by electrolysis, followed by the reaction with the organic ligand *in situ* to form metal–organic compounds for on-line MS analysis. Several intact daily-life and industry objects, including gold necklaces, fuel nozzles and bearing balls, were used to demonstrate the performance of the present method. The experimental results indicate that the key merits of this method include the high speed of analysis (less than 10 min per sample), high chemical sensitivity (LOD = 0.05 ppb for Cu), and low sample consumption (nanograms).

## 2 Experimental

Details about the materials, instruments and sample preparation can be found in the ESI.†

### 2.1 Preparation of the calibration curve for Ni<sup>2+</sup>, Cu<sup>2+</sup> and Pb<sup>2+</sup>

Standard solution: Ni(NO<sub>3</sub>)<sub>2</sub>, Cu(NO<sub>3</sub>)<sub>2</sub> and Pb(NO<sub>3</sub>)<sub>2</sub> were used as the source of Ni<sup>2+</sup>, Cu<sup>2+</sup> and Pb<sup>2+</sup>, respectively. A series of working solutions of Ni<sup>2+</sup>, Cu<sup>2+</sup> and Pb<sup>2+</sup> with different concentrations (0.2 ppb, 1 ppb, 10 ppb, 20 ppb, 50 ppb, 100 ppb, 200 ppb, 500 ppb, 1000 ppb) was prepared in 0.05 mM EDTA in H<sub>2</sub>O/CH<sub>3</sub>CN (v/v = 1/1) solution, respectively.

The experiments were performed on an Orbitrap-MS instrument (Thermo Scientific, Bremen) in a negative ion detection mode. The ESI voltage was –3 kV. The flow rate of the standard solution was 4.0 μL min<sup>-1</sup>, supplied by a syringe pump. And the same flow rate is used elsewhere in this work. The temperature of the heated capillary of the Orbitrap-MS instrument was 250 °C. The tube lens voltage was –100 V, and the capillary voltage was –30 V. Because the molecular weight of all studied metal–organic complexes is below 500, the *m/z* range was set between 50 and 500. The maximum injection time was 100 ms. These conditions were used for all the MS experiments, unless specified otherwise. The LODs of metal ions obtained by this method was calculated using the equation  $LOD = 3\sigma/a$ , where  $\sigma$  is the standard deviation of the blank solution ( $n = 7$ ) and  $a$  is the slope of the standard curve.

### 2.2 Detection of Ni, Cu and Pb in golden jewelry

The detection of Ni, Cu and Pb was carried out by electrolysis of the doped metal in 0.5 mL of 0.05 mM EDTA in H<sub>2</sub>O/CH<sub>3</sub>CN (v/v = 1/1) solution. Golden jewelry, platinum wire and Ag/AgCl were used as working electrode, counter electrode and reference electrode, respectively. A potential of +0.8 V was used to electrolyze Ni, Cu and Pb into the corresponding ions. The formed ions reacted with EDTA–2Na contained in the solution to form metal–organic compounds, which were detected by MS analysis. Before MS detection, the metals were completely transformed into metal ions by electrolysis, and the electrolysis

terminal was determined by the electrochemical signal. After MS analysis, the sample was taken out and the whole device was successively cleaned with 0.1 M HNO<sub>3</sub> and H<sub>2</sub>O until the signals of the metal–organic compounds disappeared when EDTA/H<sub>2</sub>O/CH<sub>3</sub>CN was used as electrolyte. SEM was used to characterize the change of jewelry form after analysis.

For comparison, an inductively coupled plasma optical emission spectrometer (ICP-OES) (Thermo Fisher, USA) was used for Ni, Cu and Pb determinations. The operation conditions and the wavelengths are summarized in Table S1.† Before that, HNO<sub>3</sub>/H<sub>2</sub>O (1 M) was used to dissolve the metals on the jewelry surface with the assistance of ultrasound for 20 min.

### 2.3 Analysis of the fuel nozzle

The analysis of Pb on the inner wall of the fuel nozzle was carried out by electrolyzing the metal into ions. Similarly, 0.05 mM EDTA in H<sub>2</sub>O/CH<sub>3</sub>CN (v/v = 1/1) solution was infused into the pipe of the fuel nozzle, and a drop was generated at the outlet of the pipe, which was used as an electrolytic cell. Then, the fuel nozzle, platinum wire and Ag/AgCl were used as working electrode, counter electrode and reference electrode, respectively. A potential of +0.8 V was used to electrolyze Ni, Cu and Pb into corresponding ions. The formed ions reacted with EDTA–2Na contained in the solution to form metal–organic compounds, which were detected by MS analysis.

### 2.4 Evaluation of the corrosion resistance of the bearing ball

The steel bearing ball was washed with water first. A carbon rod, Pt wire and Ag/AgCl were used as working, counter and reference electrodes, respectively. The bearing ball was placed in the electrolytic cell and connected to the working electrode in 0.05 mM EDTA in H<sub>2</sub>O/CH<sub>3</sub>CN (v/v = 1/1) solution. After having applied +0.8 V potential for 2 min, the electrolyte was collected for MS analysis. A defective bearing ball was prepared by scraping the original ball with abrasive paper. And then, the same analytical procedure was carried out to analyze the defective ball.

## 3 Results and discussion

### 3.1 Construction of the analytical device

As schematically shown in Fig. 1, experiments were carried out using an Orbitrap mass spectrometer in which an electrolytic cell was implemented without any hardware modifications.<sup>29,30</sup> The sample was placed in the electrolytic cell and connected to the working electrode (carbon rod). Platinum wire was used as a counter electrode, and Ag/AgCl was used as a reference electrode. Electrolyte solution containing the organic ligand (0.05 mM EDTA–2Na in H<sub>2</sub>O/CH<sub>3</sub>CN (v/v = 1/1) solution) was infused into the electrolytic cell containing the sample. After a potential (*e.g.* +0.8 V) floated on the ESI voltage was applied to the working electrode *via* an electrochemical workstation, the metal component on the irregular sample was transformed into metal ions.<sup>31,32</sup> The generated ions readily

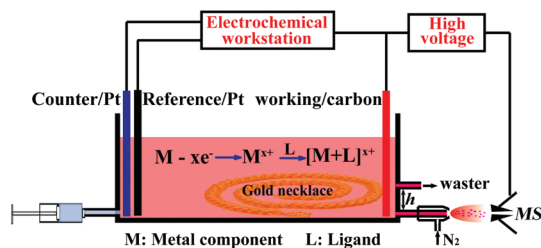


**Fig. 1** Schematic diagram of EC-MS for rapid quality and safety inspection of an irregular device by the detection of a metal component. As an example, metal component on gold jewelry can be directly detected without complex sample pretreatment.

reacted with the organic ligand to form metal–organic compounds for on-line Orbitrap-MS analysis.<sup>33,34</sup> By varying the organic ligand, the present method can provide a selective detection method for metals.<sup>26</sup> Note that the present method employs electrolysis to sample the metals. Therefore, the metals which come into contact with the electrolyte can be transformed into metal ions by applying an appropriate voltage for MS analysis, while the metals inside a sample where the electrolyte cannot come into contact would not be detected. However, some pretreatments can be employed to expose the inside metal for analysis, such as scraping, electro-etching, etc.

### 3.2 Investigation of the qualitative and quantitative performance

The qualitative and quantitative performance of the present method was investigated by preparing calibration curves for three metal ions ( $\text{Ni}^{2+}$ ,  $\text{Cu}^{2+}$  and  $\text{Pb}^{2+}$ ). A series of standard solutions was prepared by spiking different concentrations of  $\text{Ni}^{2+}$ ,  $\text{Cu}^{2+}$  and  $\text{Pb}^{2+}$  in 0.05 mM EDTA in  $\text{H}_2\text{O}/\text{CH}_3\text{CN}$  ( $v/v = 1/1$ ) solution, respectively. MS detection was performed in negative ion detection mode. As shown in Fig. 2a–c,  $[\text{Ni}^{58} + \text{EDTA-4H}]^{2-}$  ( $m/z$  172.9968)/ $[\text{Ni}^{60} + \text{EDTA-4H}]^{2-}$  ( $m/z$  173.9945) = 2.59/1,  $[\text{Cu}^{63} + \text{EDTA-4H}]^{2-}$  ( $m/z$  175.4939)/ $[\text{Cu}^{65} + \text{EDTA-4H}]^{2-}$  ( $m/z$  176.4930) = 2.25/1,  $[\text{Cu}^{63} + \text{EDTA-4H-CO}_2]^-$  ( $m/z$  306.9983)/ $[\text{Cu}^{65} + \text{EDTA-4H-CO}_2]^-$  ( $m/z$  308.9965) = 2.25/1,  $[\text{Cu}^{63} + \text{EDTA-4H-2CO}_2]^-$  ( $m/z$  263.0081)/ $[\text{Cu}^{65} + \text{EDTA-4H-2CO}_2]^-$  ( $m/z$  265.0062) = 2.24/1,  $[\text{Pb}^{206} + \text{EDTA-4H}]^{2-}$  ( $m/z$  247.0161)/ $[\text{Pb}^{208} + \text{EDTA-4H}]^{2-}$  ( $m/z$  248.0171) = 0.46/1, and  $[\text{Pb}^{207} + \text{EDTA-4H}]^{2-}$  ( $m/z$  247.5168)/ $[\text{Pb}^{208} + \text{EDTA-4H}]^{2-}$  ( $m/z$  248.0171) = 0.42/1 were observed in the mass spectra with high precision ( $\Delta m < 2.85$  ppm). Characteristic peaks of ( $[\text{Ni}^{58} + \text{EDTA-4H}]^{2-}$ ,  $[\text{Cu}^{63} + \text{EDTA-4H}]^{2-}$  and  $[\text{Pb}^{208} + \text{EDTA-4H}]^{2-}$ ) were used as the quantitative ions for  $\text{Ni}^{2+}$ ,  $\text{Cu}^{2+}$  and  $\text{Pb}^{2+}$ , respectively. After the detection of standard solutions, three calibration curves (intensity vs. concentration) of  $\text{Ni}^{2+}$ ,  $\text{Cu}^{2+}$  and  $\text{Pb}^{2+}$  were plotted, as shown in Fig. 2d, with the calibration equations. A wide linear response range of 0.1 ppb–1000 ppb with  $R^2 > 0.99$  was obtained for these three metal ions. The LODs were calculated to be 0.07 ppb for  $\text{Ni}^{2+}$ , 0.05 ppb for  $\text{Cu}^{2+}$  and 0.08 ppb for  $\text{Pb}^{2+}$  (detailed in the Experimental section).

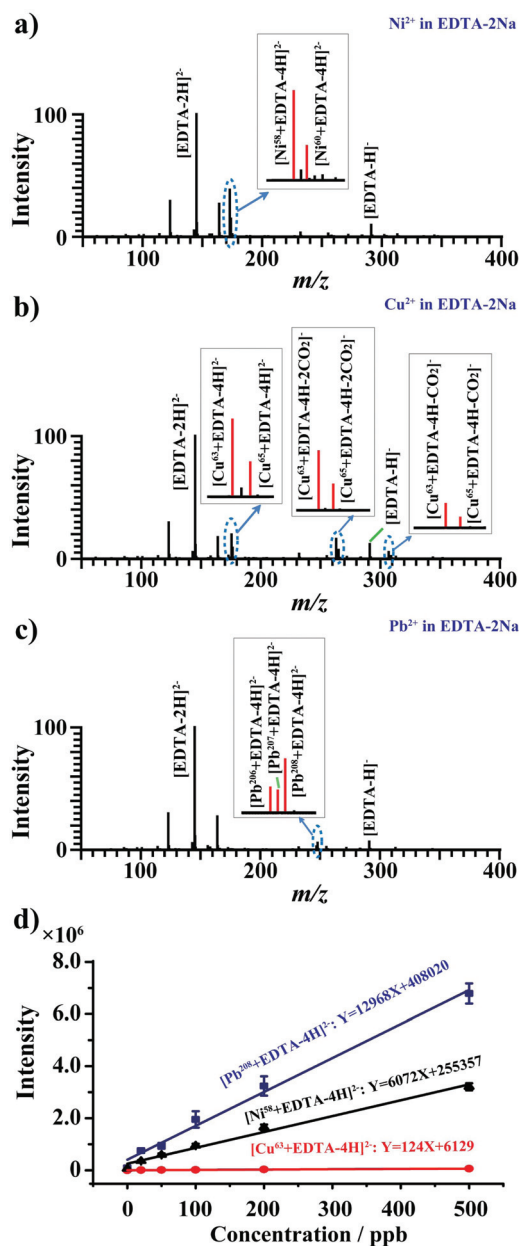


**Fig. 2** Qualitative and quantitative performance of EC-MS. (a) Mass spectrum of  $\text{Ni}^{2+}$  in 0.05 mM EDTA in  $\text{H}_2\text{O}/\text{CH}_3\text{CN}$  ( $v/v = 1/1$ ) solution; (b) mass spectrum of  $\text{Cu}^{2+}$  in 0.05 mM EDTA in  $\text{H}_2\text{O}/\text{CH}_3\text{CN}$  ( $v/v = 1/1$ ) solution; (c) mass spectrum of  $\text{Pb}^{2+}$  in 0.05 mM EDTA in  $\text{H}_2\text{O}/\text{CH}_3\text{CN}$  ( $v/v = 1/1$ ) solution; and (d) calibration curves of  $\text{Ni}^{2+}$ ,  $\text{Cu}^{2+}$  and  $\text{Pb}^{2+}$ . The error bars represent standard deviations of X replicates. The dominant peak assignments:  $m/z$  172.9965  $[\text{Ni}^{58} + \text{EDTA-4H}]^{2-}$ ;  $m/z$  175.4934  $[\text{Cu}^{63} + \text{EDTA-4H}]^{2-}$ ;  $m/z$  248.0171  $[\text{Pb}^{208} + \text{EDTA-4H}]^{2-}$ ;  $m/z$  263.0081  $[\text{Cu}^{63} + \text{EDTA-4H-2CO}_2]^-$ ;  $m/z$  291.0817  $[\text{EDTA-H}]^-$ ;  $m/z$  306.9983  $[\text{Cu}^{63} + \text{EDTA-4H-CO}_2]^-$ .

### 3.3 Quality and safety inspection of gold jewelry

The first application example is a demonstration of quality and safety inspection of gold jewelry. Some non-noble metals (e.g. Cu and Ni) are often doped in the jewelry. Especially, some heavy metals (e.g. Pb) are also used to dope in the

jewelry, which is harmful to health.<sup>7,8</sup> Thus, it is of great significance to detect the doped metal. As described in the Experimental section, Ni, Cu and Pb on a gold jewelry surface (1.59 g) were first electrolyzed into the corresponding ions in 0.05 mM EDTA in H<sub>2</sub>O/CH<sub>3</sub>CN (v/v = 1/1) solution, and then detected by MS. As shown in Fig. 3a, notable signals of [Ni + EDTA-4H]<sup>2-</sup>, [Cu + EDTA-4H]<sup>2-</sup> and [Pb + EDTA-4H]<sup>2-</sup> could be observed in the mass spectrum. According to the intensity of the MS signal and calibration equation, the amount of the doped metal was calculated to be 0.10 μg (62.59 ppb) for Ni, 0.98 μg (613.22 ppb) for Cu and 0.14 μg (85.55 ppb) for Pb. This was in good accordance with the result of 0.11 μg (62.04 ppb) for Ni, 0.94 μg (605.38 ppb) for Cu and 0.15 μg (83.27 ppb) for Pb, which was obtained with the OES method (Fig. 3b). In the US, the allowable content of lead in children's

jewelry is 100 ppm (0.01%),<sup>9</sup> which is about 1169 times higher than our detected result (85.55 ppb), indicating that our method is sufficiently sensitive for the evaluation of lead content below the regulated threshold. Because no complex sample pretreatment was required, the analysis process took only about 10 min, which is less than that in AAS, AES or ICP-MS. Compared to spot-by-spot analysis by LA-ICP-MS, this method can be used to analyze the whole sample at one time. The mass of the consumed sample was calculated to be nano-grams according to eqn (S1)–(S3),† which are detailed in the ESI.† Fig. 3c and d shows the SEM images of the gold jewelry before and after analysis. Negligible damage is seen after analysis, indicating that this method has very low invasiveness to samples, which is important for the analysis of valuable samples.

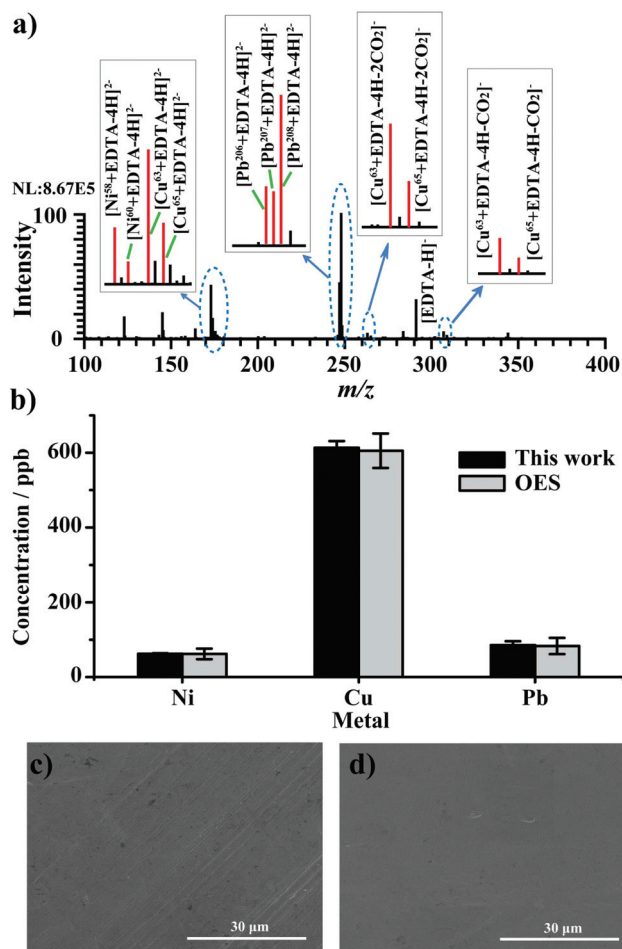


Fig. 3 Analysis of doped metal in gold jewelry. (a) Mass spectrum of the electrolyte of doped gold jewelry after electrolysis; (b) quantification results of Cu, Ni and Pb obtained by our method and OES; (c) SEM image of gold jewelry before electrolysis; and (d) SEM image of gold jewelry after electrolysis. The conditions of electrolysis are as follows: gold jewelry was used as a working electrode; platinum wire was used as a counter electrode; Ag/AgCl was used as a reference electrode; the electrolysis potential is +0.8 V; the electrolyte is 0.05 mM EDTA in H<sub>2</sub>O/CH<sub>3</sub>CN (v/v = 1/1) solution.

### 3.4 Detection of Pb on the inner wall of a fuel nozzle

Another important application of this method is quality inspection of sophisticated parts and components. For example, a fuel nozzle is an important and sophisticated component of a car, which is used for the nebulization of the fuel for higher efficiency of combustion. The materials of the fuel nozzle are stainless steel, nickel alloy or chromium alloy, *etc.* However, the use of Pb in the fuel nozzle is harmful to the environment. The inset in Fig. 4 shows the application of our method for the inner wall analysis of a fuel nozzle. 0.05 mM EDTA-2Na in H<sub>2</sub>O/CH<sub>3</sub>CN (v/v = 1/1) solution was used as the electrolyte and infused into the pipe of the fuel nozzle. Then, the fuel nozzle was used as a working electrode, platinum wire was used as a counter electrode and Ag/AgCl was used as a reference electrode. After having applied a +0.8 potential for 300 s, the doped Pb was electrolyzed into ions and then reacted with EDTA-2Na to form an EDTA-Pb compound. Fig. 4 shows the mass spectrum of the electrolyte after electrolysis and a notable signal of [Pb + EDTA-4H]<sup>2-</sup> can be observed. Note that the diameter of the fuel nozzle tube was smaller than 1 mm, while the inner wall of the tube is a hard-to-reach region for laser, X-ray or physical scraping. Therefore, the analytical results of Pb on the inner wall of the fuel nozzle indicated that the present method is a useful method for the analysis of hard-to-reach regions of the sample whereas it is

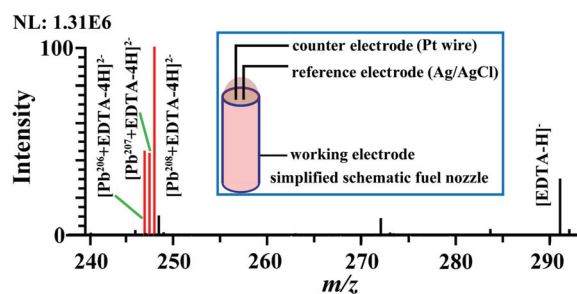


Fig. 4 Mass spectrum of the electrolyte of the Pb-doped fuel nozzle after electrolysis in 0.05 mM EDTA in H<sub>2</sub>O/CH<sub>3</sub>CN (v/v = 1/1) solution. The inset is the schematic diagram of the analysis of the fuel nozzle.

difficult for physical methods (*e.g.*, laser ablation, X-ray excitation, scraping) to sample or detect without destroying the sample.

### 3.5 Evaluation of the corrosion resistance of a bearing ball

A bearing ball is another important mechanical component with broad applications in various areas. Generally, to prevent the corrosion of a bearing ball, some treatment methods are used, such as coating with slushing oil or doping with chromium. Thus, rapid analysis of the effect of the cladding materials is important for the application of the bearing ball. The present method is well suited for analysis of the corrosion resistance of a bearing ball, because corrosion of a bearing ball is essentially a redox process.<sup>37</sup> As shown in Fig. 1, a bearing ball was placed in the electrolyte (0.05 mM EDTA-2Na in H<sub>2</sub>O/CH<sub>3</sub>CN (v/v = 1/1) solution) and connected to a

working electrode, while the Pt wire and Ag/AgCl were used as a counter electrode and a reference electrode, respectively. After having applied +0.8 V potential, the electrolyte was collected for MS analysis. As shown in Fig. 5a, almost no signal of Fe was detected from the original bearing ball, indicating that this bearing ball has good resistance to corrosion. After that, hexamethylene and acetonitrile were used to remove the slushing oil on the bearing surface with the assistance of ultrasound.

As can be seen in Fig. 5b, the signal of Fe was still almost undetectable even though the slushing oil was removed, indicating that this bearing ball still has a remainder of protective layer to resist corrosion. Further damage was made to the bearing ball by scraping the ball's surface with abrasive paper (Fig. 5d and e). A scraped area of about 3 mm × 3 mm was generated. The same analytical conditions were used for the scraped bearing ball analysis. A notable signal of ([Fe<sup>54</sup> + EDTA-4H]<sup>-</sup>) and Fe ([Fe<sup>56</sup> + EDTA-4H]<sup>-</sup>) with a ratio of 0.06 : 1 could be observed in the mass spectrum at this time (Fig. 5c),<sup>19</sup> indicating the corrosion of the scraped bearing ball. Thus, our method is also useful for the evaluation of the corrosion resistance of metal samples.

## 4 Conclusions

In summary, we report an electrochemical mass spectrometry method for the direct detection of metal impurities on various intact objects that are widely used in daily life and industry. This method features a high speed of analysis (less than 10 min per sample), high sensitivity (LOD = 0.05 ppb), low sample consumption (nanograms level) and minimal sample invasiveness. The unique feature of this method is that even metal (*e.g.*, Pb, Ni) localized on hard-to-reach tiny spots on the inner surface of extremely irregular shapes can be detected. By using this method, metal impurities (*e.g.*, Cu, Ni, Pb) on several typical samples, including gold necklaces, fuel nozzles, and bearing balls, were detected successfully. Our results demonstrate that the present method is a promising method for the quality and safety inspection of various objects with irregular shapes with regard to the occurrence of metal impurities in food safety, environmental monitoring, mechanical manufacturing and other areas.

## Conflicts of interest

There are no conflicts to declare.

## Acknowledgements

This work was supported by the National Natural Science Foundation of China (no. 21705016, 21727812, 21605017), the Program for Changjiang Scholars and Innovative Research Team in University (PCSIRT) (no. IRT\_17R20), the Science and Technology Planning Project at the Department of Science and

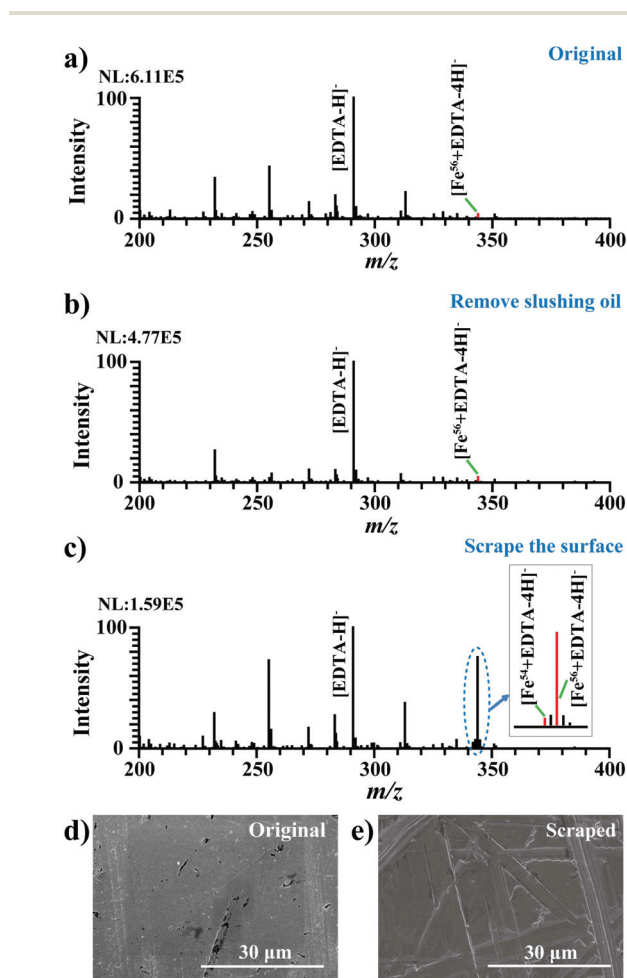


Fig. 5 Evaluation of the effect of the cladding material on the bearing ball. (a) Mass spectrum of the electrolyte of the original bearing ball after electrolysis; (b) mass spectrum of the electrolyte of the bearing ball from which the slushing oil was removed; (c) mass spectrum of the electrolyte of the bearing ball after the surface was scraped; (d) SEM image of the surface of the original bearing ball; (e) SEM image of the scraped surface of the bearing ball. The dominant peak of [Fe<sup>56</sup> + EDTA-4H]<sup>-</sup> was *m/z* 343.9934.

Technology of Jiangxi Province (no. 20171ACB21046), and the Project of the Jiangxi Provincial Department of Education (no. GJJ160543).

## References

- 1 I. Milosev, *Pure Appl. Chem.*, 2011, **83**, 309–324.
- 2 C. M. Doherty, D. Buso, A. J. Hill, S. Furukawa, S. Kitagawa and P. Falcaro, *Acc. Chem. Res.*, 2014, **47**, 396–405.
- 3 B. Y. Xia, H. B. Wu, N. Li, Y. Yan, X. W. Lou and X. Wang, *Angew. Chem., Int. Ed.*, 2015, **54**, 3797–3801.
- 4 S. Das and A. Engineering, *Int. J. Sci. Res. Publ.*, 2014, **4**, 1–12.
- 5 C. C. Merriman, D. F. Bahr and M. G. Norton, *Gold Bull.*, 2005, **38**, 113–119.
- 6 J. D. Weidenhamer and M. L. Clement, *Chemosphere*, 2007, **67**, 961–965.
- 7 D. J. Gawkrödger, F. M. Lewis and M. J. Shah, *Am. Acad. Dermatol.*, 2000, **43**, 31–36.
- 8 R. P. Maas, S. C. Patch, T. J. Pandolfo, J. L. Druhan and N. F. B. Gandy, *Environ. Contam. Toxicol.*, 2005, **74**, 437–444.
- 9 M. Guney and G. J. Zagury, *Environ. Sci. Technol.*, 2012, **46**, 4265–4274.
- 10 S. L. C. Ferreira, M. A. Bezerra, A. S. Santos, W. N. L. dos Santos, C. G. Novaes, O. M. C. de Oliveira, M. L. Oliveira and R. L. Garcia, *TrAC, Trends Anal. Chem.*, 2018, **100**, 1–6.
- 11 S. J. Hill, *Chem. Soc. Rev.*, 1997, **26**, 291–298.
- 12 E. H. Evans, S. Chenery, A. Fisher, J. Marshall and K. J. Sutton, *Anal. At. Spectrom.*, 1999, **14**, 977–1004.
- 13 P. Pohl, *TrAC, Trends Anal. Chem.*, 2004, **23**, 87–101.
- 14 D. Beauchemin, *Anal. Chem.*, 2010, **82**, 4786–4810.
- 15 T. Minami, W. Konagaya, L. Zheng, S. Takano, M. Sasaki, R. Murata, Y. Nakaguchi and Y. Sohrin, *Anal. Chim. Acta*, 2015, **854**, 183–190.
- 16 B. Hattendorf, C. Latkoczy and D. Günther, *Anal. Chem.*, 2003, **75**, 341–347A.
- 17 R. Huang, Y. Quan, L. Li, Y. Lin, H. Wei, H. Jian and B. Huang, *Mass Spectrom. Rev.*, 2011, **30**, 1256–1268.
- 18 B. Fernández, F. Claverie, C. Péchevran, O. F. X. Donard and F. Claverie, *TrAC, Trends Anal. Chem.*, 2007, **26**, 951–966.
- 19 C. Shiea, Y. L. Huang, S. C. Cheng, Y. L. Chen and J. Shiea, *Anal. Chim. Acta*, 2017, **968**, 50–57.
- 20 M. K. Van, A. Smekens, M. Behets, P. Kazandjian and G. R. Van, *Anal. Chem.*, 2007, **79**, 6383–6389.
- 21 V. Rößiger and B. Nensel, *Gold Bull.*, 2003, **36**, 125–137.
- 22 R. Cesareo, A. Brunetti and S. Ridolfi, *X-Ray Spectrom.*, 2008, **37**, 309–316.
- 23 P. Y. Liu, M. Lu, Q. L. Zheng, Y. Zhang, H. D. Dewald and H. Chen, *Analyst*, 2013, **138**, 5519–5539.
- 24 T. A. Brown, H. Chen and R. N. Zare, *J. Am. Chem. Soc.*, 2015, **137**, 7274–7277.
- 25 T. A. Brown, N. Hosseini-Nassab, H. Chen and R. N. Zare, *Chem. Sci.*, 2016, **7**, 329–332.
- 26 J. Q. Xu, T. G. Zhu, K. Chingin, Y. H. Liu, H. Zhang and H. W. Chen, *Anal. Chem.*, 2018, **90**, 13832–13836.
- 27 S. Luo, X. Mi, L. Zhang, S. Liu, H. Xu and J. P. Cheng, *Angew. Chem., Int. Ed.*, 2006, **45**, 3093–3097.
- 28 J. Boeser, H. P. Permentier, A. P. Bruins and R. Bischoff, *Anal. Chem.*, 2010, **82**(18), 7556–7565.
- 29 F. Zhou and G. J. V. Berkel, *Anal. Chem.*, 1995, **67**, 3643–3649.
- 30 F. T. G. van den Brink, W. Olthuis, A. van den Berg and M. Odijk, *TrAC, Trends Anal. Chem.*, 2015, **70**, 40–49.
- 31 K. Ogle and S. J. Weber, *Electrochem. Soc.*, 2000, **147**, 1770–1780.
- 32 A. Y. Li, Q. J. Luo, S. J. Park and R. G. Cooks, *Angew. Chem.*, 2014, **126**, 3211–3214.
- 33 E. C. K. And and J. S. Brodbelt, *Anal. Chem.*, 2000, **72**, 5411–5416.
- 34 G. J. V. Berkel, K. G. Asano and P. D. Schnier, *J. Am. Soc. Mass Spectrom.*, 2001, **12**, 853–862.
- 35 Z. L. Chen, Q. Sun, Y. F. Xi and G. Owens, *J. Sep. Sci.*, 2008, **31**, 3796–3802.
- 36 Z. Chen, G. Owens, K. R. Kim and R. Naidu, *Anal. Chim. Acta*, 2007, **599**, 163–169.
- 37 N. Perez, *Electrochemistry and Corrosion Science*, Springer US, 2004.